

Heavy Quark Photoproduction in Coherent Interactions at High Energies

V.P. Gonçalves¹, M.V.T. Machado², A.R. Meneses¹

¹ Instituto de Física e Matemática, Universidade Federal de Pelotas
Caixa Postal 354, CEP 96010-090, Pelotas, RS, Brazil

² Centro de Ciências Exatas e Tecnológicas, Universidade Federal do Pampa
Campus de Bagé, Rua Carlos Barbosa. CEP 96400-970. Bagé, RS, Brazil

We calculate the inclusive and diffractive photoproduction of heavy quarks in proton-proton collisions at Tevatron and LHC energies, where the photon reaches energies larger than those ones accessible at DESY-HERA. The integrated cross section and the rapidity distributions for charm and bottom production are computed within the color dipole picture employing three phenomenological saturation models based on the Color Glass Condensate formalism. Our results demonstrate that the experimental analyzes of these reactions is feasible and that the cross sections are sensitive to the underlying parton dynamics.

PACS numbers: 25.75.Dw, 13.60.Le

I. INTRODUCTION

The cross sections for heavy quark production in hadron-hadron and lepton-hadron collisions at high energies are strongly dependent on the behavior of the gluon distribution, which is determined by the underlying QCD dynamics (See e.g. Refs. [1, 2]). Theoretically, at high energies the QCD evolution leads to a system with high gluon density, characterized by the limitation on the maximum phase-space parton density that can be reached in the hadron wavefunction (parton saturation). The transition is specified by a typical scale, which is energy dependent and is called saturation scale Q_{sat} (For recent reviews see Ref. [3]). Signals of parton saturation have already been observed both in ep deep inelastic scattering at HERA and in deuteron-gold collisions at RHIC (See, e.g. Ref. [4]). In particular, in Ref. [5] we demonstrated that the inclusive charm total cross section exhibits the property of geometric scaling, which is one of the main characteristics of the high density approaches. However, the observation of this new regime still needs confirmation and so there is an active search for new experimental signatures. In this paper we study the inclusive and diffractive photoproduction of heavy quarks in proton-proton collisions considering three phenomenological models based on the Color Glass Condensate, which describe quite well the current experimental HERA data for inclusive and exclusive observables. Our goal is twofold: update our previous studies [6, 7] considering these new parameterizations for the dipole scattering amplitude and present a comparison between the inclusive and diffractive production mechanisms using an identical theoretical input.

Our main motivation comes from the fact that in coherent interactions at Tevatron and LHC the photon reaches energies higher than those currently accessible at DESY - HERA. In hadron-hadron colliders, the relativistic protons give rise to strong electromagnetic fields, which can interact with each other. Namely, quasi-real photons scatters off protons at very high energies in the current hadron colliders (For recent reviews on coherent interactions see, e.g., Ref. [8]). In particular, the heavy quark photoproduction cross section in a proton-proton collision is given by,

$$\sigma(p + p \rightarrow p + Q\bar{Q} + Y) = 2 \int_0^\infty \frac{dN_\gamma(\omega)}{d\omega} \sigma_{\gamma p \rightarrow Q\bar{Q}Y} \left(W_{\gamma p}^2 = 2\omega \sqrt{S_{NN}} \right) d\omega, \quad (1)$$

where ω is the photon energy in the center-of-mass frame (c.m.s.), $W_{\gamma p}$ is the c.m.s. photon-proton energy and $\sqrt{S_{NN}}$ denotes the proton-proton c.m.s.energy. The final state Y can be a hadronic state generated by the fragmentation of one of the colliding protons (inclusive production) or a proton (diffractive production). The photon spectrum is given by [9],

$$\frac{dN_\gamma(\omega)}{d\omega} = \frac{\alpha_{\text{em}}}{2\pi\omega} \left[1 + \left(1 - \frac{2\omega}{\sqrt{S_{NN}}} \right)^2 \right] \left(\ln \Omega - \frac{11}{6} + \frac{3}{\Omega} - \frac{3}{2\Omega^2} + \frac{1}{3\Omega^3} \right), \quad (2)$$

with the notation $\Omega = 1 + [(0.71 \text{ GeV}^2)/Q_{\text{min}}^2]$ and $Q_{\text{min}}^2 = \omega^2/[\gamma_L^2(1 - 2\omega/\sqrt{S_{NN}})] \approx (\omega/\gamma_L)^2$, where γ_L is the Lorentz factor. The expression above is derived considering the Weizsäcker-Williams method of virtual photons and using an elastic proton form factor (For more detail see Refs. [9, 10]). It is important to emphasize that the expression (2) is based on a heuristic approximation, which leads to an overestimation of the cross section at high energies ($\approx 11\%$ at $\sqrt{s} = 1.3 \text{ TeV}$) in comparison with the more rigorous derivation of the photon spectrum for elastic scattering on protons derived in Ref. [11]. For a more detailed comparison among the different photon spectra see Ref. [12]. As a photon stemming from the electromagnetic field of one of the two colliding protons can interact with one photon

of the other proton (two-photon process) or can interact directly with the other proton (photon-hadron process), both possibilities have been studied in the literature. In principle, the experimental signature of these two processes is distinct and it can easily be separated. While in two-photon interactions we expect the presence of two rapidity gaps and no hadron breakup, in the inclusive heavy quark photon-hadron production the hadron target we expect only one rapidity gap and the dissociation of the hadron. However, as shown in Ref. [7], the diffractive heavy quark photoproduction, where we also expect the presence of two rapidity gaps in the final state, similarly to two-photon interactions, is an important background for two-photon interactions as well as for the dedicated program to search evidence of the Higgs and/or new physics in central double diffractive production processes [13].

In what follows, we briefly review the description of the inclusive and diffractive photoproduction of heavy quarks within the dipole picture and the distinct phenomenological saturation models which will be used in our calculations (Section II). Our results are compared with the DESY-HERA data [14] and the predictions from the bCGC and IP-SAT models for this process are presented for the first time. In Section III the numerical results for the rapidity y of the produced states and their total cross sections are shown. A comparison on the order of magnitude of the cross sections for the distinct models is performed. Finally in Section IV we present our main conclusions.

II. QCD DIPOLE PICTURE AND SATURATION MODELS

The photon-hadron interaction at high energy (small x) is usually described in the infinite momentum frame of the hadron in terms of the scattering of the photon off a sea quark, which is typically emitted by the small- x gluons in the proton. However, in order to describe inclusive and diffractive interactions and disentangle the small- x dynamics of the hadron wavefunction, it is more adequate to consider the photon-hadron scattering in the dipole frame, in which most of the energy is carried by the hadron, while the photon has just enough energy to dissociate into a quark-antiquark pair before the scattering. In this representation the probing projectile fluctuates into a quark-antiquark pair (a dipole) with transverse separation \mathbf{r} long after the interaction, which then scatters off the target [15]. The main motivation to use this color dipole approach, is that it gives a simple unified picture of inclusive and diffractive processes. In particular, in this approach the inclusive heavy quark photoproduction cross section [$\gamma p \rightarrow Q\bar{Q}X$] reads as,

$$\sigma_{tot}(\gamma p \rightarrow Q\bar{Q}X) = 2 \int d^2\mathbf{b} \int d^2\mathbf{r} \int dz \Psi_\gamma^*(\mathbf{r}, z) \mathcal{N}(x, \mathbf{r}, \mathbf{b}) \Psi_\gamma(\mathbf{r}, z) . \quad (3)$$

Furthermore, the diffractive cross section for the process $\gamma p \rightarrow Q\bar{Q}p$ is given by

$$\sigma_{tot}^D(\gamma p \rightarrow Q\bar{Q}p) = \int d^2\mathbf{b} \int d^2\mathbf{r} \int dz \Psi_\gamma^*(\mathbf{r}, z) \mathcal{N}^2(x, \mathbf{r}, \mathbf{b}) \Psi_\gamma(\mathbf{r}, z) . \quad (4)$$

In the Eqs. (3) and (4) the variable \mathbf{r} defines the relative transverse separation of the pair (dipole), z ($1 - z$) is the longitudinal momentum fractions of the quark (antiquark) and the function $\Psi_\gamma(\mathbf{r}, z)$ is the light-cone wavefunction for transversely polarized photons, which depends in our case of the charge (e_Q) and mass (m_Q) of the heavy quark and is given by

$$|\Psi_\gamma(\mathbf{r}, z)|^2 = \frac{6\alpha_{em}}{4\pi^2} e_Q^2 \{ [z^2 + (1-z)^2] m_Q^2 K_1^2(m_Q \mathbf{r}) + m_Q^2 K_0^2(m_Q \mathbf{r}) \} . \quad (5)$$

The function $\mathcal{N}(x, \mathbf{r}, \mathbf{b})$ is the forward dipole-target scattering amplitude for a dipole with size \mathbf{r} and impact parameter \mathbf{b} which encodes all the information about the hadronic scattering, and thus about the non-linear and quantum effects in the hadron wave function (see e.g. [3]). It can be obtained by solving the BK (JIMWLK) evolution equation in the rapidity $Y \equiv \ln(1/x)$. Many groups have studied the numerical solution of the BK equation, but several improvements are still necessary before using the solution in the calculation of observables. In particular, one needs to include the next-to-leading order corrections into the evolution equation and perform a global analysis of all small x data. It is a program in progress (for recent results see [16, 17]). In the meantime it is necessary to use phenomenological models for \mathcal{N} which capture the most essential properties of the solution.

During the last years an intense activity in the area resulted in sophisticated models for the dipole-proton scattering amplitude, which have strong theoretical constraints and which are able to describe the HERA and/or RHIC data [18, 19, 20, 21, 22, 23, 24, 25, 26, 27, 28]. In what follows we will use three distinct phenomenological saturation models based on the Color Glass Condensate which describe quite well the more recent HERA data: the IIM [21], the bCGC [22, 24] and the IP-SAT model [20, 22, 24]. In the IIM model [21] the scattering amplitude $\mathcal{N}(x, \mathbf{r}, \mathbf{b})$ was constructed to smoothly interpolate between the limiting behaviors analytically under control: the solution of the BFKL equation for small dipole sizes, $\mathbf{r} \ll 1/Q_{sat}(x)$, and the Levin-Tuchin law [29] for larger ones, $\mathbf{r} \gg 1/Q_{sat}(x)$. Moreover, the authors have assumed that the impact parameter dependence can be factorized: $\mathcal{N}(x, \mathbf{r}, \mathbf{b}) = \mathcal{N}(x, \mathbf{r})S(\mathbf{b})$. A fit to the

structure function $F_2(x, Q^2)$ was performed in the kinematical range of interest, showing that it is not very sensitive to the details of the interpolation (For details see e.g [6]). The predictions of this model for several observables were studied in Refs. [6, 30, 31, 32]. Recently the IIM model was improved by the inclusion of the impact parameter dependence in the scattering amplitude, with the resulting model being usually denoted bCGC. The parameters of this model were fitted to describe the current HERA data in Ref. [24]. Following [22] we have that the dipole-proton scattering amplitude is given by:

$$\mathcal{N}^{\text{bCGC}}(x, \mathbf{r}, \mathbf{b}) = \begin{cases} \mathcal{N}_0 \left(\frac{r Q_s}{2} \right)^{2\left(\gamma_s + \frac{\ln(2/r Q_s)}{\kappa \lambda Y}\right)} & r Q_s \leq 2 \\ 1 - \exp^{-A \ln^2(B r Q_s)} & r Q_s > 2 \end{cases} \quad (6)$$

with $Y = \ln(1/x)$ and $\kappa = \chi''(\gamma_s)/\chi'(\gamma_s)$, where χ is the LO BFKL characteristic function. The coefficients A and B are determined uniquely from the condition that $\mathcal{N}(x, \mathbf{r})$ and its derivative with respect to $r Q_s$ are continuous at $r Q_s = 2$. In this model, the proton saturation scale Q_s now depends on the impact parameter:

$$Q_s \equiv Q_s(x, \mathbf{b}) = \left(\frac{x_0}{x} \right)^{\frac{1}{\lambda}} \left[\exp \left(-\frac{\mathbf{b}^2}{2B_{\text{CGC}}} \right) \right]^{\frac{1}{2\gamma_s}}. \quad (7)$$

The parameter B_{CGC} was adjusted to give a good description of the t -dependence of exclusive J/ψ photoproduction. Moreover the factors \mathcal{N}_0 and γ_s were taken to be free. In this way a very good description of F_2 data was obtained. The parameter set which is going to be used here is the one presented in the second line of Table II of [24]: $\gamma_s = 0.46$, $B_{\text{CGC}} = 7.5 \text{ GeV}^{-2}$, $\mathcal{N}_0 = 0.558$, $x_0 = 1.84 \times 10^{-6}$ and $\lambda = 0.119$. Furthermore, we will use in our calculations the scattering amplitude scattering proposed in Ref. [22], denoted IP-SAT, which is given by

$$\mathcal{N}^{\text{IP-SAT}}(x, \mathbf{r}, \mathbf{b}) = \left[1 - \exp \left(-\frac{\pi^2}{2N_c} \mathbf{r}^2 \alpha_s(\mu^2) x g(x, \mu^2) T(\mathbf{b}) \right) \right], \quad (8)$$

where the scale μ^2 is related to the dipole size \mathbf{r} by $\mu^2 = 4/\mathbf{r}^2 + \mu_0^2$ and the gluon density is evolved from a scale μ_0^2 up to μ^2 using LO DGLAP evolution without quarks assuming that the initial gluon density is given by $xg(x, \mu_0^2) = A_g x^{-\lambda_g} (1-x)^{5.6}$. The values of the parameters μ_0^2 , A_g and λ_g are determined from a fit to F_2 data. Moreover, it is assumed that the proton shape function $T(\mathbf{b})$ has a Gaussian form, $T(\mathbf{b}) = 1/(2\pi B_G) \exp[-(\mathbf{b}^2/2B_G)]$, with B_G being a free parameter which is fixed by the fit to the differential cross sections for exclusive vector meson production. The parameter set used in our calculations is the one presented in the first line of Table III of [22]: $\mu_0^2 = 1.17 \text{ GeV}^2$, $A_g = 2.55$, $\lambda_g = 0.020$ and $B_G = 4 \text{ GeV}^{-2}$.

As discussed in Refs. [33, 34] the expression (8) for the forward scattering amplitude can be obtained to leading logarithmic accuracy in the classical effective theory of the Color Glass Condensate formalism. Moreover, it is applicable when the leading logarithms in Q^2 dominate the leading logarithms in $1/x$, with the small \mathbf{r} limit being described by the linear DGLAP evolution at small- x . In contrast, the bCGC model for \mathcal{N} , Eq. 6, captures the basic properties of the quantum evolution in the CGC formalism, describing both the bremsstrahlung limit of linear small- x evolution (BFKL equation) as well nonlinear renormalization group at high parton densities (very small- x). Consequently, the IP-SAT model can be considered a phenomenological model for the classical limit of the CGC, while the bCGC for the quantum limit. It is important to emphasize that both models provide excellent fits to a wide range of HERA data for $x \leq 0.01$. Therefore, the study of observables which are strongly dependent on \mathcal{N} is very important to constrain the underlying QCD dynamics at high energies. In what follows we consider these two models as input in our calculations of the inclusive and diffractive heavy quark photoproduction in γp collisions at HERA and coherent pp interactions at Tevatron and LHC energies. For comparison we also consider the IIM model [21].

Having presented the phenomenological models which will be used in our calculations, in Fig. 1 we compare the numerical results for the inclusive heavy quark photoproduction with the experimental DESY-HERA data [14]. In all calculations we have use the same quark masses $m_c = 1.4 \text{ GeV}$ and $m_b = 4.5 \text{ GeV}$. We quote Ref. [6] for a comparison of the experimental data with another theoretical approaches. In order to describe the threshold region, $W \rightarrow 2m_Q$, we have multiplied the cross sections by a factor $(1-x)^7$, following studies presented in Ref. [35]. In charm case (left panel), the IIM and bCGC predictions are almost identical in all kinematical range. In contrast, the predictions for these two models for bottom production differ at small energy. The IP-SAT predictions are approximately a factor 2 larger than the IIM and bCGC predictions. One have that the IIM and bCGC models underestimate the experimental data for charm production at high energies, producing a reasonable description of the region near threshold (low energies: $W \leq 20 \text{ GeV}$). In contrast, the IP-SAT model describes the high energy region but overestimate the low energy regime. For the bottom case, the value of x which determines the magnitude of the saturation scale is not sufficiently small, which implies that the cross section is dominated by the linear regime of the scattering amplitude. The three models give a reasonable description of the scarce experimental data. Unfortunately,

	$Q\bar{Q}$	IIM	bCGC	IP-SAT
Tevatron	$c\bar{c}$ (incl.)	1230 nb	1245 nb	2310 nb
	$c\bar{c}$ (diff.)	37 nb	49 nb	114 nb
	$b\bar{b}$ (incl.)	11 nb	10 nb	32 nb
	$b\bar{b}$ (diff.)	0.04 nb	0.08 nb	0.30 nb
LHC	$c\bar{c}$ (incl.)	3821 nb	3662 nb	7542 nb
	$c\bar{c}$ (diff.)	165 nb	161 nb	532 nb
	$b\bar{b}$ (incl.)	51 nb	51 nb	158 nb
	$b\bar{b}$ (diff.)	0.32 nb	0.52 nb	3 nb

TABLE I: The integrated cross section for the inclusive and diffractive photoproduction of heavy quarks in $pp(\bar{p})$ collisions at Tevatron and LHC energies.

the current precision and statistics of the experimental measurements of the photoproduction cross section are either low to formulate definitive conclusions about the robustness of the different saturation models presented here. More precise measurements could be pose stringent constraints on the energy dependence and overall normalization. Finally, it should be noticed that the present calculations concern only the direct photon contribution to the cross section, whereas the resolved component has been neglected. In some extent the results from the saturation models presented here let some room for this contribution. Details on its calculation and size of its contribution can be found, for instance, in Ref. [36].

In Fig. 2 we present our predictions for the diffractive photoproduction of heavy quarks. In comparison with the inclusive case, the diffractive cross sections are approximately a factor 30 smaller. The main aspect is that the difference between the saturations models is enlarged, which is directly associated to the quadratic dependence of the cross section on the scattering amplitude. It implies that the experimental study of these observables can be useful to determine the QCD dynamics at high energies.

III. RESULTS

In what follows, we will compute the rapidity distribution and total cross sections for the inclusive and diffractive photoproduction of heavy quarks from proton-proton collisions at high energies. The phenomenological models shortly reviewed in the previous section serve as input for the numerical calculations using Eq. (1) for the energies of the current and future pp and $p\bar{p}$ accelerators. Namely, one considers the Tevatron value $\sqrt{S_{NN}} = 1.96$ TeV for its $p\bar{p}$ running and for the planned LHC pp running one takes the design energy $\sqrt{S_{NN}} = 14$ TeV.

The distribution on rapidity y of the produced open heavy quark state can be directly computed from Eq. (1), by using its relation with the photon energy ω , i.e. $y \propto \ln(\omega/m_Q)$. A reflection around $y = 0$ takes into account the interchanging between the proton's photon emitter and the proton target. Explicitly, the rapidity distribution is written down as,

$$\frac{d\sigma [p + p \rightarrow p + Q\bar{Q} + Y]}{dy} = \omega \frac{N_\gamma(\omega)}{d\omega} \sigma_{\gamma p \rightarrow Q\bar{Q}Y}(\omega), \quad (9)$$

where Y is a hadronic final state X resulting of the proton fragmentation in the inclusive case and $Y = p$ for diffractive production.

The resulting rapidity distributions for inclusive and diffractive heavy quark photoproduction coming out of the distinct phenomenological models considered in previous section are depicted in Figs. (3-6) at Tevatron and LHC energies. For the inclusive case (Figs. 3 and 5) the IIM and bCGC predictions are very similar, as expected from the analyzes at photon level in the previous section. In contrast, these predictions are distinct in the diffractive case, with the bCGC prediction being larger than IIM one at mid-rapidity. On the other hand, the IP-SAT prediction is larger than these predictions by a factor 2 (3) in the charm (bottom) case. We can consider the IIM and bCGC predictions as a lower bound for the coherent production of heavy quarks at Tevatron and LHC. Our results indicate that the experimental study of the inclusive heavy quark photoproduction can be very useful to discriminate between the classical and quantum versions of the CGC formalism. It also is true in the diffractive case, where the different models can be discriminated more easily.

Let us now compute the integrated cross section considering the distinct phenomenological models. The results are presented in Table I, for the inclusive and diffractive charm and bottom pair production at Tevatron and LHC. The

IP-SAT model gives the largest rates among the approaches studied, followed by the bCGC and IIM models with almost identical predictions, as a clear trend from the distribution on rapidity. In the inclusive case, the values are either large at Tevatron and LHC, going from some units of nanobarns at Tevatron to microbarns at LHC. Therefore, these reactions can have high rates at the LHC kinematical regime. On the other hand, the cross sections for diffractive production are approximately two orders of magnitude smaller than the inclusive case, but due the clear experimental signature of this process (two rapidity gaps), its experimental analyzes still is feasible.

In comparison with our previous results for the inclusive production of heavy quarks [6] we have that our predictions using the modern phenomenological IIM and bCGC models are similar. However, the IP-SAT prediction is factor of ≈ 2 larger. In the diffractive case, our predictions are larger by a factor $\gtrsim 2$ than those presented in [7], where we have used the GBW model [18] as input in our calculations. This behavior is directly associated to the different energy dependence predicted by the models for the linear regime. Furthermore, in comparison with the predictions for the heavy quark hadroproduction (See e.g. [37]), photoproduction cross sections are smaller ($\lesssim 1\%$). However, the experimental separation between these two mechanics is feasible due to the presence of one rapidity gap in the photoproduction process.

Lets now calculate the production rates for charm and bottom production in coherent interactions. At Tevatron, assuming the design luminosity $\mathcal{L}_{\text{Tevatron}} = 2 \times 10^{32} \text{ cm}^{-2}\text{s}^{-1}$, we have for inclusive production of charm $2 - 4 \times 10^2$ and for bottom $2 - 6$ events/second. In the diffractive case, we predict $7 - 22$ ($8 - 60 \times 10^{-3}$) events/second for charm (bottom) production. At LHC, where $\mathcal{L}_{\text{LHC}} = 10^{34} \text{ cm}^{-2}\text{s}^{-1}$, we predict for inclusive (diffractive) charm production $38 - 75 \times 10^3$ ($16 - 52 \times 10^2$) and for bottom $5 - 15 \times 10^2$ ($3 - 30$) events/second. Notice the large rate for bottom at LHC.

Finally, lets discuss the experimental separation of the inclusive and diffractive photoproduction of heavy quarks. As emphasized in Refs. [6, 7, 10], although the inclusive photoproduction cross section to be a small fraction of the hadronic cross section, the separation of this channel is feasible if we impose the presence of a rapidity gap in the final state. It occurs due to the proton which is the photon emitter remains intact in the process. We expect that a cut in the transverse momentum of the pair could eliminate most part of the contribution associated to the hadroproduction of heavy quarks. Moreover, in comparison with the hadroproduction of heavy quarks, the event multiplicity for photoproduction interactions is lower, which implies that it may be used as a separation factor between these processes. In the case of diffractive photoproduction of heavy quarks we expect the presence of two rapidity gaps in the final state, similarly to two-photon or Pomeron-Pomeron interactions. Consequently, it is important to determine the magnitude of this cross section in order to estimate the background for these other channels. In particular, the central exclusive diffraction (CED) process characterized by the production of a final state via fusion of two Pomerons has being intensely studied as an alternative process to search evidence of the Higgs and/or new physics [13], with the main background being the exclusive $b\bar{b}$ production. In Ref. [38], the double diffractive (DD) heavy quark production is studied using the diffractive factorization theorem, including absorption corrections. The magnitude of the cross section is the following: for Tevatron one has $\sigma_{c\bar{c}}^{\text{DD}} \simeq 4.6 \mu\text{b}$ and $\sigma_{b\bar{b}}^{\text{DD}} \simeq 0.1 \mu\text{b}$, whereas for the LHC one obtains $\sigma_{c\bar{c}}^{\text{DD}} \simeq 18 \mu\text{b}$ and $\sigma_{b\bar{b}}^{\text{DD}} \simeq 0.5 \mu\text{b}$. It is expected that emerging protons from CED and DD processes have a much larger transverse momentum than those resulting from diffractive photoproduction processes. Consequently, in principle it is possible to introduce a selection criteria to separate these two processes. However, this subject deserves more detailed studies.

IV. CONCLUSIONS

In summary, we have computed the cross sections for inclusive and diffractive photoproduction of heavy quarks in $p\bar{p}$ and pp collisions at Tevatron and LHC energies, respectively. This has been performed using modern phenomenological models based on the Color Glass Condensate formalism, which describe quite well the inclusive and exclusive observables measured in ep collisions at HERA. The obtained values are shown to be sizeable at Tevatron and are increasingly larger at LHC. The feasibility of detection of these reactions is encouraging, since their experimental signature should be suitably clear. Furthermore, they enable to constrain the underlying QCD dynamics at high energies, which is fundamental to predict the observables which will be measured in central hadron-hadron collisions at LHC.

Acknowledgments

This work was partially financed by the Brazilian funding agencies CNPq and FAPERGS.

-
- [1] M. Bedjidian *et al.*, arXiv:hep-ph/0311048.
 - [2] V. P. Goncalves and M. V. T. Machado, Mod. Phys. Lett. A **19**, 2525 (2004).
 - [3] E. Iancu and R. Venugopalan, arXiv:hep-ph/0303204; A. M. Stasto, Acta Phys. Polon. B **35**, 3069 (2004); H. Weigert, Prog. Part. Nucl. Phys. **55**, 461 (2005); J. Jalilian-Marian and Y. V. Kovchegov, Prog. Part. Nucl. Phys. **56**, 104 (2006).
 - [4] J. P. Blaizot and F. Gelis, Nucl. Phys. A **750**, 148 (2005).
 - [5] V. P. Goncalves and M. V. T. Machado, Phys. Rev. Lett. **91**, 202002 (2003); JHEP **0704**, 028 (2007).
 - [6] V. P. Goncalves and M. V. T. Machado, Phys. Rev. D **71**, 014025 (2005).
 - [7] V. P. Goncalves and M. V. T. Machado, Phys. Rev. D **75**, 031502 (2007).
 - [8] G. Baur, K. Hencken, D. Trautmann, S. Sadovsky, Y. Kharlov, Phys. Rep. **364**, 359 (2002); C. A. Bertulani, S. R. Klein and J. Nystrand, Ann. Rev. Nucl. Part. Sci. **55**, 271 (2005).
 - [9] M. Drees and D. Zeppenfeld, Phys. Rev. D **39**, 2536 (1989).
 - [10] S. R. Klein and J. Nystrand, Phys. Rev. Lett. **92**, 142003 (2004).
 - [11] B. A. Kniehl, Phys. Lett. B **254**, 267 (1991).
 - [12] J. Nystrand, arXiv:hep-ph/0412096.
 - [13] V. A. Khoze, A. D. Martin and M. G. Ryskin, Eur. Phys. J. C **23**, 311 (2002)
 - [14] J. Breitweg *et al.* [ZEUS Collaboration], Eur. Phys. J. C **6**, 67 (1999);
C. Adloff *et al.* [H1 Collaboration], Nucl. Phys. B **545**, 21 (1999);
J. Breitweg *et al.* [ZEUS Collaboration], Eur. Phys. J. C **12**, 35 (2000);
J.J. Aubert *et al.* [European Muon Collaboration], Phys. Lett. B **106**, 419 (1981);
C. Adloff *et al.* [H1 Collaboration], Phys. Lett. B **467**, 156 (1999) [Erratum-ibid. B **518**, 331 (2001)];
J. Breitweg *et al.* [ZEUS Collaboration], Eur. Phys. J. C **18**, 625 (2001).
 - [15] N. N. Nikolaev and B. G. Zakharov, Z. Phys. **C49**, 607 (1991); Z. Phys. **C53**, 331 (1992); A. H. Mueller, Nucl. Phys. **B415**, 373 (1994); A. H. Mueller and B. Patel, Nucl. Phys. **B425**, 471 (1994).
 - [16] J. L. Albacete, Phys. Rev. Lett. **99**, 262301 (2007).
 - [17] J. L. Albacete, N. Armesto, J. G. Milhano and C. A. Salgado, arXiv:0902.1112 [hep-ph].
 - [18] K. Golec-Biernat and M. Wüsthoff, Phys. Rev. D **60**, 114023 (1999); Phys. Rev. D **59**, 014017 (1998).
 - [19] J. Bartels, K. Golec-Biernat and H. Kowalski, Phys. Rev. D **66** (2002) 014001.
 - [20] H. Kowalski and D. Teaney, Phys. Rev. D **68**, 114005 (2003).
 - [21] E. Iancu, K. Itakura, S. Munier, Phys. Lett. B **590**, 199 (2004).
 - [22] H. Kowalski, L. Motyka and G. Watt, Phys. Rev. D **74**, 074016 (2006).
 - [23] C. Marquet, R. B. Peschanski and G. Soyez, Phys. Rev. D **76**, 034011 (2007)
 - [24] G. Watt and H. Kowalski, Phys. Rev. D **78**, 014016 (2008).
 - [25] D. Kharzeev, Y.V. Kovchegov and K. Tuchin, Phys. Lett. **B599**, 23 (2004).
 - [26] A. Dumitru, A. Hayashigaki and J. Jalilian-Marian, Nucl. Phys. **A765**, 464 (2006); Nucl. Phys. **A770**, 57 (2006).
 - [27] V. P. Goncalves, M. S. Kugeratski, M. V. T. Machado and F. S. Navarra, Phys. Lett. B **643**, 273 (2006).
 - [28] D. Boer, A. Utermann and E. Wessels, Phys. Rev. D **77**, 054014 (2008).
 - [29] E. Levin and K. Tuchin, Nucl. Phys. B **573**, 833 (2000).
 - [30] J. R. Forshaw, R. Sandapen and G. Shaw, JHEP **0611**, 025 (2006).
 - [31] M.V.T. Machado, Eur. Phys. J. C **47**, 365 (2006).
 - [32] V. P. Goncalves and M. V. T. Machado, Eur. Phys. J. C **37**, 299 (2004).
 - [33] H. Kowalski, T. Lappi and R. Venugopalan, Phys. Rev. Lett. **100**, 022303 (2008) .
 - [34] H. Kowalski, T. Lappi, C. Marquet and R. Venugopalan, Phys. Rev. C **78**, 045201 (2008).
 - [35] A. Szczurek, Eur. Phys. J. C **26**, 183 (2002).
 - [36] L. Motyka, N. Timneanu, Eur. Phys. J. C **27**, 73 (2003).
 - [37] J. Raufeisen and J. C. Peng, Phys. Rev. D **67**, 054008 (2003).
 - [38] M.V.T. Machado, Phys. Rev. D **76**, 054006 (2007).

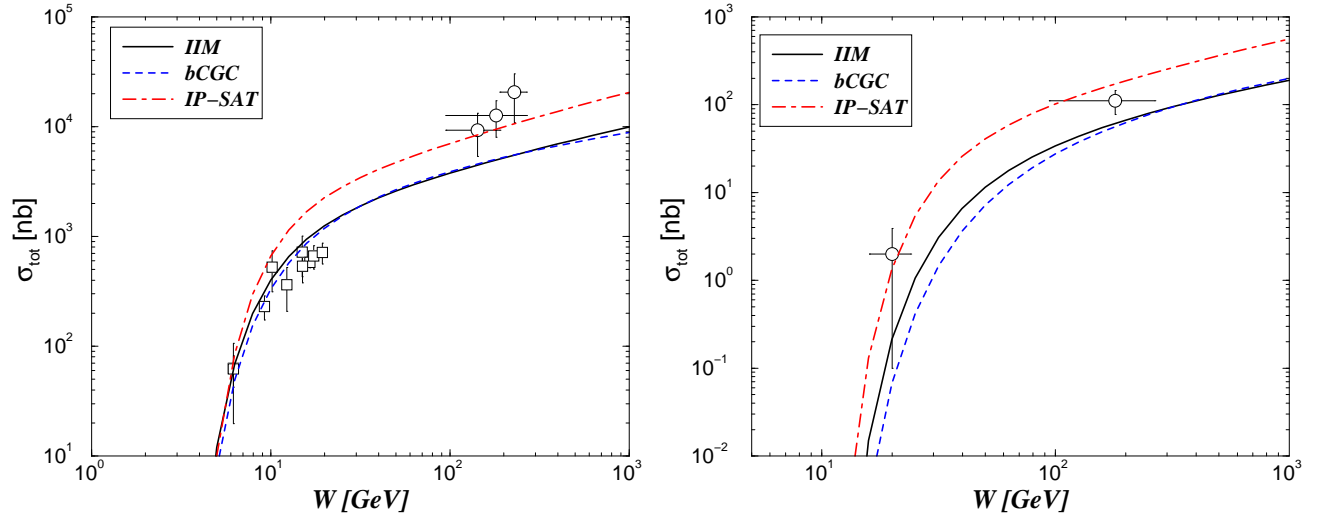


FIG. 1: The total photoproduction cross section for charm (left panel) and bottom (right panel). The experimental measurements are from DESY-HERA.

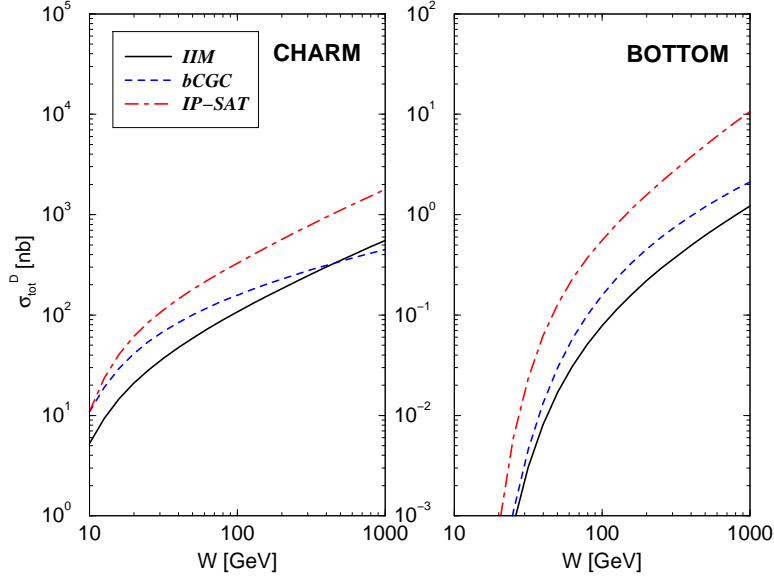


FIG. 2: The energy dependence of the diffractive cross section for the charm (left panel) and bottom (right panel) production predicted by the distinct phenomenological models.

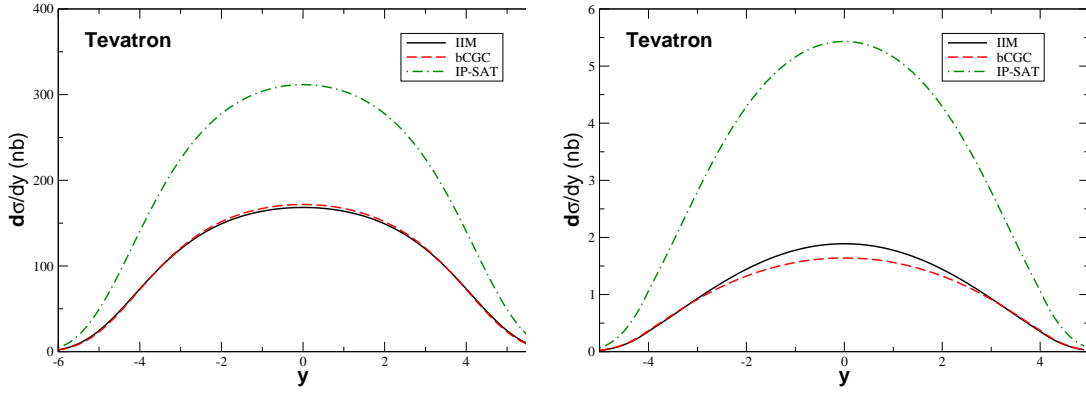


FIG. 3: The rapidity distribution for the inclusive charm (left panel) and bottom (right panel) photoproduction on pp reactions at Tevatron energy $\sqrt{S_{NN}} = 1.96$ TeV. Different curves correspond to distinct phenomenological models.

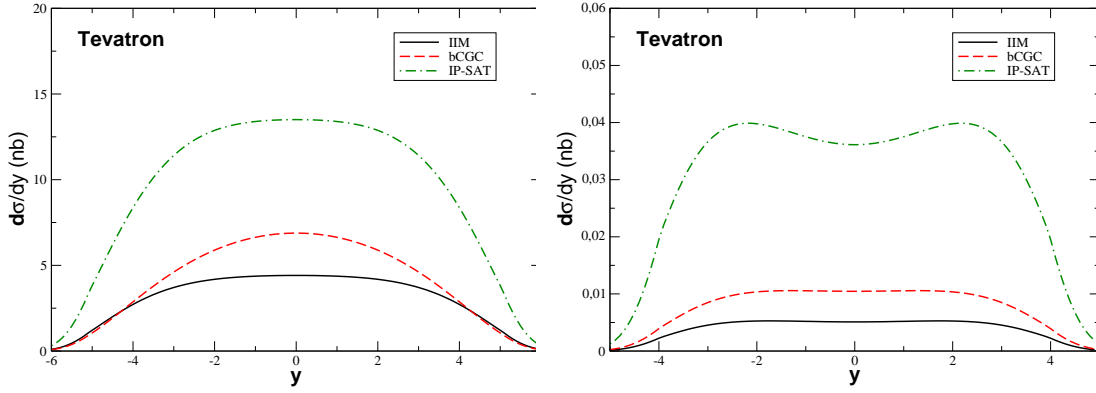


FIG. 4: The rapidity distribution for the diffractive charm (left panel) and bottom (right panel) photoproduction on $p\bar{p}$ reactions at Tevatron energy $\sqrt{S_{NN}} = 1.96$ TeV. Different curves correspond to distinct phenomenological models.

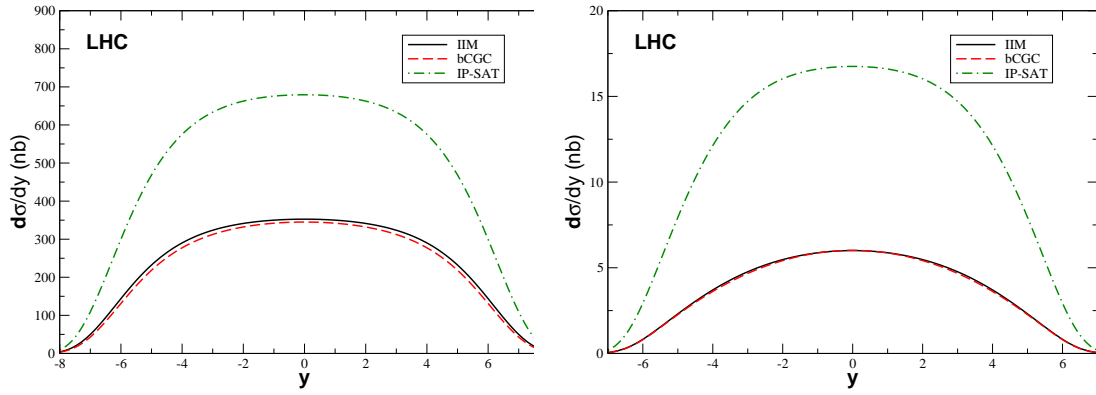


FIG. 5: The rapidity distribution for the inclusive charm (left panel) and bottom (right panel) photoproduction on $p\bar{p}$ reactions at LHC energy $\sqrt{S_{NN}} = 14$ TeV. Different curves correspond to distinct phenomenological models.

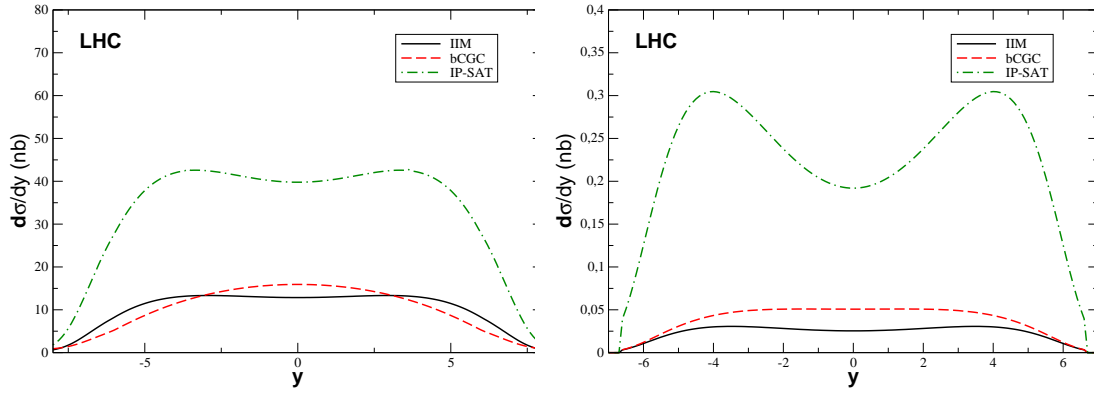


FIG. 6: The rapidity distribution for the diffractive charm (left panel) and bottom (right panel) photoproduction on $p\bar{p}$ reactions at LHC energy $\sqrt{S_{NN}} = 14$ TeV. Different curves correspond to distinct phenomenological models.